LETTERS TO THE EDITOR

The Letters to the Editor section is divided into four categories entitled Communications, Notes, Comments, and Errata. Communications are limited to three and one half journal pages, and Notes, Comments, and Errata are limited to one and three-fourths journal pages as described in the Announcement in the 1 July 1995 issue.

COMMUNICATIONS

Photoelectron–neutral–neutral coincidence studies of dissociative photodetachment

K. A. Hanold, C. R. Sherwood, and R. E. Continetti
Department of Chemistry and Biochemistry, University of California, San Diego, 9500 Gilman Drive, La Jolla, California 92093-0314

(Received 29 August 1995; accepted 6 October 1995)

Photoelectron–neutral–neutral coincidence spectra have been measured for the dissociative photodetachment of O_4^- ($O_4^- + h\nu \rightarrow O_2 + O_2 + e^-$) at 523 and 349 nm. The neutral photofragment translational energy spectrum, the photoelectron spectrum, and the correlations of the translational energy and photoelectron energy are presented here. The correlation spectra reveal phenomena that are not discernable in either one-dimensional measurement. Features are observed which indicate that non-Franck–Condon processes play a role in the dissociative photodetachment of O_4^- at 349 nm. © *1995 American Institute of Physics.*

The study of mass- and energy-selected transient neutral species remains an important research area in chemical physics. One approach to studying transient neutral molecules and free radicals involves photodetachment of mass-selected negative-ion beams.[1] Photoelectron spectroscopy of negative ions has revealed a great deal about the electronic and vibrational structure of anions and transient neutral molecules,[2] and has even provided a novel route to the study of the transition-state region for neutral bimolecular reactions.[3] When photodetachment takes place into multiple continua, i.e., the nascent neutral dissociates, more information may be obtained by performing an experiment in which both the photoelectron and the photofragments are recorded in coincidence. We have performed this measurement for the first time in a study of the dissociative photodetachment (DPD) of the tetroxide ion, O_4^-.

Previous studies have shown that O_4^- undergoes both photodissociation and photodetachment over a wide range of wavelengths.[4–7] Photoelectron spectroscopy of O_4^- has produced broad spectra, significantly perturbed from that found for O_2^-.[6,7] Our laboratory has previously studied the energy and angular distributions of the neutral photofragments from the DPD of O_4^- at 523 nm,[8] however, the partitioning of the kinetic energy between the photoelectron and the photofragments was not determined in these earlier experiments. This Letter presents the correlation of the electron kinetic energy with the translational energy of the photofragments in the DPD of O_4^- ($O_4^- + h\nu \rightarrow O_2 + O_2 + e^-$) at 523 and 349 nm, providing new insights into the dynamics of this process.

The experiments described here make use of translational energy spectroscopy and photoelectron spectroscopy in a fast negative-ion beam. A schematic of the experimental geometry is shown in Fig. 1. A brief description of the apparatus follows—a more detailed description can be found in Refs. 8–10. Anions are produced and cooled in a pulsed free-jet expansion of O_2 intersected by a 1 keV electron beam. The anions are accelerated to a kinetic energy of 4 keV and mass selected by time-of-flight. Anions at the mass of interest are intersected by a pulsed linearly polarized laser beam (Spectra Physics TFR). The laser pulse is 6 ns full width at half maximum and is focused to a spot of ≈0.5 mm diameter at the interaction region. The fundamental output of the Nd:YLF (1047 nm) was doubled and tripled using standard nonlinear optical techniques to make 523 (180 μJ/pulse) and 349 (20 μJ/pulse) nm light.

The photoelectron spectrometer[9] uses a paraboloidal electrostatic mirror[11,12] to cover 80% of 4π sr and uses a time- and position-sensitive detector to allow correction for the Doppler broadening from the fast-ion-beam velocity. The mirror reflects electrons which are emitted off axis of the electron spectrometer drift tube. The detector uses a wedge-and-strip anode[13] to record the time and position of arrival of the electron. The spectrometer has been calibrated using photoelectrons from 4 keV I^- at 349 nm, giving an energy resolution of $\Delta E/E \leqslant 35\%$ at 0.5 eV.

The translational energy spectrometer is similar to that used by Neumark and co-workers to study free-radical

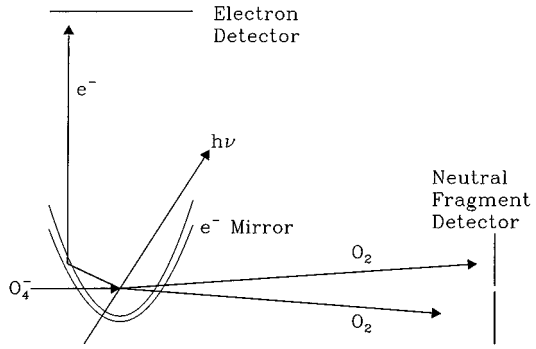

FIG. 1. Schematic of the experimental geometry. The photoelectron is collected and energy-analyzed using a paraboloidal electrostatic mirror, while the two O_2 photofragments produced in the DPD of O_4^- are detected in coincidence, yielding photofragment translational energy and angular distributions.

 0021-9606/95/103(22)/9876/4/$6.00 © 1995 American Institute of Physics
Downloaded 04 Apr 2002 to 132.239.157.211. Redistribution subject to AIP license or copyright, see http://ojps.aip.org/jcpo/jcpcr.jsp

dissociation.[1] Photofragments recoil out of the beam as they traverse the 96 cm flight path between the laser interaction and the photofragment detector. The photofragments that clear a 5 mm wide beam block impinge on a 40 mm diameter time- and position-sensitive microchannel plate detector. This detector makes use of two side-by-side wedge-and-strip anodes to record the time and position of arrival for each of the photofragments. Detector calibration was performed using photodissociation of O_2^- at 262 nm indicating an energy resolution of $\Delta E/E \approx 10\%$ at 0.62 eV.[8]

The photoelectron and both O_2 photofragments from the O_4^- DPD were detected in coincidence on an event-by-event basis. Residual ions and ionic photofragments were removed from the beam by electrostatic deflection after the laser interaction region. Since each detector can only detect one photofragment per laser pulse, the photodestruction rate was held to ≈0.2 event per shot. To overcome this low event rate the apparatus was run at 600 Hz.

For each coincident pair of photofragments, the center-of-mass (CM) for that event was calculated. The CM was required to have the same time and position of arrival as that of the parent ion beam. This important discriminator allows false photofragment coincidences to be effectively eliminated. Coincidence between the photoelectron and the neutral photofragments is determined by the spectrometer detection efficiency and the count rate. A straightforward statistical calculation indicates that with the spectrometer running at 600 Hz, with a data acquisition rate of ≈3 Hz, false photoelectron–neutral fragment coincidences constitute less than 5% of the triple coincidence data.

The data presented consist only of coincident events which include an electron and two neutral photofragments. The detection of the photofragments and photoelectron in coincidence allows the determination of the masses, translational energy release, electron kinetic energy, and the recoil angles for each particle for each dissociation event.[1] No products were detected corresponding to either $O_4 + e^-$ or $O + O_3 + e^-$.

The correlation between the translational energy release and the electron kinetic energy for $O_4^- + h\nu \rightarrow O_2 + O_2 + e^-$ at 523 and 349 nm are shown as the gray-scale correlation spectra in Figs. 2(a) and 2(b), respectively. The one-dimensional projections of the correlation (i.e., the photofragment translational energy spectrum and the photoelectron kinetic energy spectrum) are shown along the x and y axes of each figure. Thresholds have been marked on Figs. 2(a) and 2(b) corresponding to the maximum translational energy available for each energetically allowed combination of electronic states for the two O_2 photofragments and the photoelectron. If it is assumed that internal energy in the parent O_4^- is negligible, the maximum translational energy release for a given product channel is given by

$$E_{T,\max} = E_{h\nu} - E_{O_2} - (\mathrm{EA} + D_0(O_2 - O_2)).$$

In this equation, $E_{h\nu}$ is the photon energy, E_{O_2} is the sum of the electronic energy in the two product O_2 molecules, EA is the electron affinity of O_4, and $D_0(O_2 - O_2)$ is the bond dissociation energy of O_4 into two ground-state O_2 molecules. The sum $\mathrm{EA} + D_0(O_2 - O_2)$ was determined from the

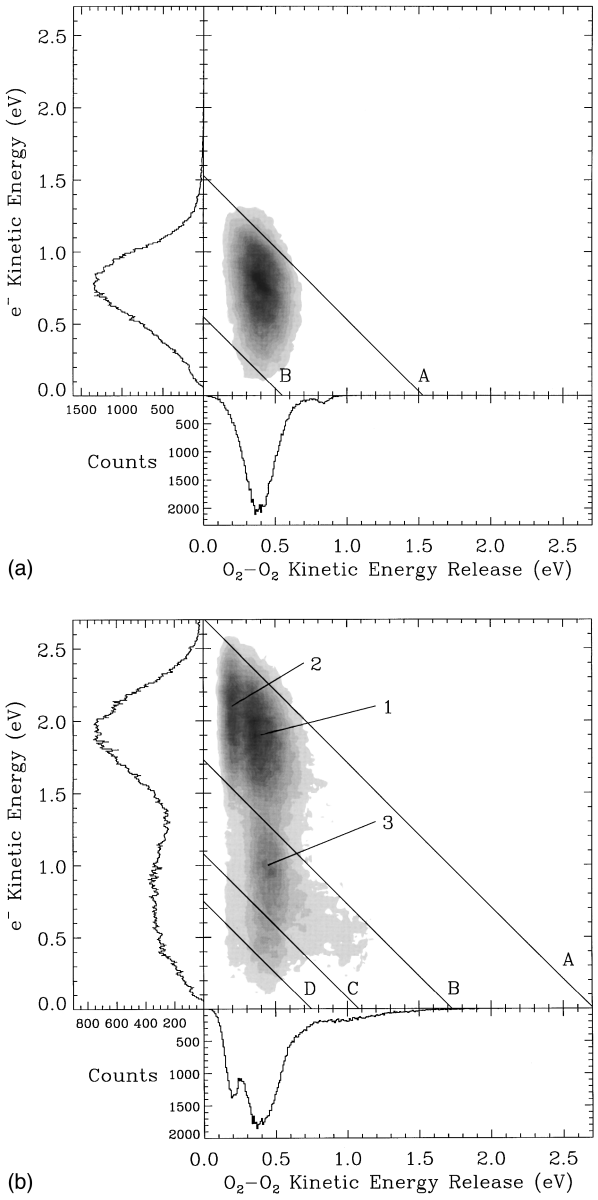

FIG. 2. (a) Correlation spectrum of the photoelectron electron kinetic energy and the translational energy release for O_4^- at 523 nm. Contours are linearly scaled, with the intensity representing the number of coincident events. The one-dimensional projections of the correlation are shown along each axis. Energetic thresholds are shown for (A) $O_2(^3\Sigma_g^-) + O_2(^3\Sigma_g^-) + e^-$ and (B) $O_2(^3\Sigma_g^-) + O_2(^1\Delta_g) + e^-$. (b) Correlation spectrum of the photoelectron kinetic energy and the translational energy release for O_4^- at 349 nm. Additional energetic thresholds are shown for (C) $O_2(^3\Sigma_g^-) + O_2(^1\Sigma_g^+) + e^-$ and (D) $O_2(^1\Delta_g) + O_2(^1\Delta_g) + e^-$. Features 1, 2, and 3 are discussed in the text.

bond dissociation energy for $O_4^- \rightarrow O_2^-(^2\Pi_g) + O_2(^3\Sigma_g^-)$ $[D_0(O_2^- - O_2) = 0.39 \pm 0.05$ eV],[10] and the electron affinity of O_2 (0.45 eV).[14]

The photofragment angular distributions were also studied for each feature in Figs. 2(a) and 2(b). The measured angular distributions were corrected for the limited detector acceptance by a grid-based direct inversion technique.[1] An electric dipole transition was assumed, the angular distributions were fit to $P(E_T, \theta) = P(E_T)[1 + \beta(E_T) P_2(\cos\theta)]$,[15] and the anisotropy parameter β describing the angular distri-

Downloaded¬04¬Apr¬2002¬to¬132.239.157.211. Redistribution subject to AIP license or copyright,¬see¬http://ojps.aip.org/jcpo/jcpcr.jsp

bution of the O_2 products was extracted. No significant dependence of the O_2 product angular distribution on the photoelectron kinetic energy was observed at 523 nm. The value at the peak is $\beta=-0.8$, which is consistent with our previous work.[8] At 349 nm, photofragment angular distributions were generated for photoelectron energies both from 0 to 1.3 eV and above 1.3 eV. This yielded the anisotropy parameters β at the peaks labeled 1, 2, and 3 in Fig. 2(b) of 0.2, 1.3, and 1.3, respectively.

The DPD of O_4^- at 523 nm shows a single broad peak in both the photoelectron spectrum and the translational energy release spectrum. The correlation spectrum also shows only one feature. This peak corresponds to production of both O_2 molecules in the $X(^3\Sigma_g^-)$ ground state. The small feature at 0.82 eV in the neutral translational energy spectrum has been shown to correspond to photodissociation of $O_4^- \rightarrow O_2^-(^2\Pi_g)+O_2(^1\Delta_g)$, followed by photodetachment of O_2^- by a second photon.[8] The photoelectron energy distribution coincident with this peak (not visible in the linearly scaled correlation spectrum) is the photoelectron spectrum for O_2^- at 523 nm.

At 349 nm, there are two peaks in both the photoelectron spectrum and the translational energy release spectrum. These pairs of peaks become three distinct peaks in the correlation spectrum. The most surprising result is that the data show two peaks in the region where only $O_2(^3\Sigma_g^-)+O_2(^3\Sigma_g^-)+e^-$ products are allowed. Peak 1 appears to be related to the single peak that was observed at 523 nm. The centroid of the translational energy is the same for both peaks and the photoelectron energy is increased by the difference between the photon energies. This peak can be simply explained within the Franck–Condon approximation for photodetachment. Peak 2, however, is characterized by a lower translational energy and a slightly higher photoelectron energy. Since there is no peak in the 523 nm data at this translational energy, it is impossible to account for this peak within the Franck–Condon approximation. The angular distribution of photofragments from peak 2 is identical to that from peak 3 which appears below the $O_2(^3\Sigma_g^-)+O_2(^1\Delta_g)+e^-$ threshold. This suggests that an exit–channel interaction between the electron and the nascent $O_2(^1\Delta_g)$ that would be produced in peak 3 results in a higher kinetic energy electron, an $O_2(^3\Sigma_g^-)$, and a lower translational energy release, yielding peak 2. Peak 2 cannot arise from a two-photon process resulting from photodissociation and then photodetachment as there is no photodissociation channel that leads to this translational energy and the photoelectron energy is not consistent with the photodetachment of O_2^- at 349 nm. In addition, no laser power dependence was observed in the translational energy release spectra.

The Franck–Condon-related peaks at 523 and 349 nm have very different photofragment angular distributions. Given the highly anisotropic angular distribution for the O_2 products at 523 nm ($\beta=-0.8$), it is clear that dissociation is occurring rapidly on the time scale of complex rotation. It is likely that the dissociation is equally rapid at 349 nm, even though β is only 0.2 at this wavelength. These features presumably result from the same electronic transition. The large change in β may arise from the fact that DPD is inherently a three-body dissociation and the angular momentum carried away by the photoelectron is generally energy dependent.[16] Similar effects have been seen in the related processes of dissociative photoionization,[17] fluorescence polarization after photoionization,[18,19] and dissociative electron-impact phenomena.[20]

The photodissociation of O_4^- throughout this wavelength range and the presence of the non-Franck–Condon features observed at 349 nm, however, indicate that DPD in O_4^- can proceed by other mechanisms as well. Numerous resonances have been found in low-energy electron–O_2 scattering experiments by Schulz and co-workers.[21] The $A(^2\Pi_u)$ state of O_2^- is expected to lie $\approx$3.1 eV above O_2^- $X(^2\Pi_g)$.[22] It is possible that a perturbed analog of this state is imbedded in the $O_2+O_2+e^-$ continuum in the energy regime reached at 349 nm. In this picture, the non-Franck–Condon feature may reveal the branching ratio for the decay of an electron–molecule scattering resonance or autodetaching state into two product channels.

Alternatively, an ion–molecule scattering interaction occurring as O_4^- evolves toward $O_2^-+O_2$ products on a repulsive ionic surface may explain the non-Franck–Condon feature at 349 nm. Resonant charge transfer is thought to play an important role in the photodissociation of symmetric dimer anions.[23] Charge-transfer photodissociation followed by a "Penning detachment"[24] reaction, $O_2^-(^2\Pi_g)+O_2(^1\Delta_g) \rightarrow O_2(^3\Sigma_g^-)+O_2(^3\Sigma_g^-)+e^-$, in the exit channel could then be invoked to explain a non-Franck–Condon process. Such a process would have to occur very early in the separation of the photofragments, however, as the kinetic-energy release between the photofragments is much lower than that observed for stable photodissociation products and a large kinetic energy is carried off by the photoelectron. The Penning detachment reaction cited above is known to have a large rate constant, and is thought to play a role in determining the free-electron density in the ionosphere.[25]

The photoelectron–neutral–neutral coincidence spectra presented here provide a measurement of the total translational energy released in the dissociation photodetachment of O_4^-. A comparison of the results at 523 and 349 nm indicates that both Franck–Condon and non-Franck–Condon processes may be occurring. Extension of these experiments to other wavelengths and the determination of photoelectron–neutral–neutral recoil vector correlations are underway and should provide new insights into the dynamics of DPD, as well as a route to the measurement of molecular-frame photoelectron angular distributions.[26] A better theoretical understanding of these dynamics will require a treatment of the half-collision interaction of the departing electron and the dissociating molecular core, as well as a consideration of competing ionic photodissociation processes. The photoelectron–neutral–neutral coincidence technique should provide the experimental impetus for theoretical developments in these areas, as well as providing a novel approach to the study of mass- and energy-selected transient neutral species.

This work was supported by the National Science Foundation. R.E.C. gratefully acknowledges the Camille and Henry Dreyfus Foundation for a New Faculty Award, the

Downloaded¬04¬Apr¬2002¬to¬132.239.157.211. Redistribution subject to AIP license or copyright,¬see¬http://ojps.aip.org/jcpo/jcpcr.jsp

David and Lucile Packard Foundation for a 1994 Fellowship in Science and Engineering and helpful conversations with Professor M. A. Johnson.

[1] R. E. Continetti, D. R. Cyr, D. L. Osborn, D. J. Leahy, and D. M. Neumark, J. Chem. Phys. **99**, 2616 (1993).
[2] K. M. Ervin and W. C. Lineberger, in *Advances in Gas Phase Ion Chemistry*, edited by N. G. Adams and L. M. Babcock (JAI, Greenwich, CT, 1992), Vol. 1.
[3] D. M. Neumark, Acc. Chem. Res. **26**, 33 (1993).
[4] L. C. Lee and G. P. Smith, J. Chem. Phys. **70**, 1727 (1979).
[5] P. C. Cosby, R. A. Bennett, J. R. Peterson, and J. T. Moseley, J. Chem. Phys. **63**, 1612 (1975).
[6] L. A. Posey, M. J. DeLuca, and M. A. Johnson, Chem. Phys. Lett. **131**, 170 (1986).
[7] M. J. DeLuca, C. C. Han, and M. A. Johnson, J. Chem. Phys. **93**, 268 (1990); C.-C. Han and M. A. Johnson, Chem. Phys. Lett. **189**, 460 (1992).
[8] C. R. Sherwood, M. C. Garner, K. A. Hanold, K. M. Strong, and R. E. Continetti, J. Chem. Phys. **102**, 6949 (1995).
[9] K. A. Hanold, C. R. Sherwood, M. C. Garner, and R. E. Continetti, Rev. Sci. Instrum. (in press).
[10] R. E. Continetti, C. R. Sherwood, M. C. Garner, K. A. Hanold, and K. M. Strong, Proc. SPIE **2548**, 122 (1995); C. R. Sherwood, K. A. Hanold, K. M. Strong, M. C. Garner, and R. E. Continetti (unpublished).
[11] D. J. Trevor, L. D. Van Woerkom, and R. R. Freeman, Rev. Sci. Instrum. **60**, 1051 (1989).
[12] J. Steadman and J. A. Syage, Rev. Sci. Instrum. **64**, 3094 (1993).
[13] C. Martin, P. Jelinsky, M. Lampton, R. F. Malina, and H. O. Anger, Rev. Sci. Instrum. **52**, 1067 (1981).
[14] M. J. Travers, D. C. Cowles, and G. B. Ellison, Chem. Phys. Lett. **164**, 449 (1989).
[15] R. N. Zare, Mol. Photochem. **4**, 1 (1972); R. Bersohn and S. H. Lin, Adv. Chem. Phys. **16**, 67 (1969); S.-C. Yang and R. Bersohn, J. Chem. Phys. **61**, 4400 (1974).
[16] J. Cooper and R. N. Zare, J. Chem. Phys. **48**, 942 (1968).
[17] J. L. Dehmer and D. Dill, Phys. Rev. A **18**, 164 (1978).
[18] C. H. Greene and R. N. Zare, Annu. Rev. Phys. Chem. **33**, 119 (1982).
[19] E. D. Poliakoff, J. L. Dehmer, D. Dill, A. C. Parr, K. H. Jackson, and R. N. Zare, Phys. Rev. Lett. **46**, 907 (1981).
[20] R. J. Van Brunt and L. J. Kieffer, Phys. Rev. A **2**, 1293 (1970); **2**, 1899 (1970).
[21] D. Spence and G. J. Schulz, Phys. Rev. A **2**, 1802 (1970); S. F. Wong, M. J. W. Boness, and G. J. Schulz, Phys. Rev. Lett. **31**, 969 (1973).
[22] K. P. Huber and G. Herzberg, *Molecular Spectra and Molecular Structure IV. Constants of Diatomic Molecules* (Van Nostrand Reinhold, New York, 1979), p. 506.
[23] P. B. Comita and J. I. Brauman, J. Am. Chem. Soc. **109**, 7591 (1987).
[24] B. Blaney and R. S. Berry, Phys. Rev. A **3**, 1349 (1970).
[25] F. C. Fehsenfeld, D. L. Albritton, J. A. Burt, and H. I. Schiff, Can. J. Chem. **47**, 1793 (1969); B. L. Upschute, W. J. Marinelli, and B. D. Green, J. Phys. Chem. **98**, 837 (1994).
[26] D. Dill, J. Chem. Phys. **65**, 1130 (1976); D. J. Leahy, K. L. Reid, and R. N. Zare, *ibid.* **95**, 1757 (1991); I. Powis, Chem. Phys. Lett. **189**, 473 (1992).

Downloaded¬04¬Apr¬2002¬to¬132.239.157.211. Redistribution subject to AIP license or copyright,¬see¬http://ojps.aip.org/jcpo/jcpcr.jsp